Investigation of the Structures of Native and Denatured Conformations of $tRNA^{Leu}_3$ by High-Resolution Nuclear Magnetic Resonance†

David R. Kearns,* Yeng P. Wong, Simon H. Chang, and Erin Hawkins

ABSTRACT: The high-resolution 300-MHz proton nuclear magnetic resonance (nmr) spectra of native (N) and denatured (D) conformers of yeast $tRNA^{Leu}_3$ have been examined over a range of temperatures. An analysis of possible base-pairing schemes was then used in conjunction with a semiempirical ring current shift theory to analyze the nmr spectra. In the native conformer there are 21 ± 2 base pairs and from an analysis of the spectra we find that the cloverleaf model provides the best description of the nmr data. The cloverleaf model also gives a consistent interpretation of the temperature dependence of the nmr spectra in terms of sequential "melting" of stems of the cloverleaf. Based on these data the DHU stem is the first to melt and the amino acid acceptor stem is the last to melt. A number of different models for the denatured conformer were examined, but only two gave a satisfactory account of the nmr spectra of the D conformer and the D–N difference spectrum. In the favored model, only the amino acid stem, and TψC stem and the minor stem from the cloverleaf model are retained, and a new helix is formed by pairing bases from the anticodon loop with bases in the TψC loop. With this model it is possible to (i) give a good account of the low-field nmr spectrum of the D conformer, (ii) predict the D–N difference spectrum, and (iii) account for the sequential melting of the D conformer observed in the nmr spectra. Some tertiary structural features for both the native and denatured conformers can be deduced from the nmr spectra.

Of the various tRNA species that have been isolated and sequenced, yeast $tRNA^{Leu}_3$ is particularly interesting since it can exist in a biologically active (the native or N conformer) and an inactive (the denatured, D conformer) state (Henley *et al.*, 1966; Fresco *et al.*, 1966; Lindahl *et al.*, 1966, 1967; Uhlenbeck *et al.*, 1972; Webb and Fresco, 1973; Gartland and Sueoka, 1966). Yeast $tRNA^{Leu}_3$, and other renaturable species that have been discovered, provide interesting systems for examining some of the unsolved structure–function problems and consequently they have been the objects of a number of investigations (Henley *et al.*, 1966; Fresco *et al.*, 1966; Lindahl *et al.*, 1966, 1967; Uhlenbeck *et al.*, 1972; Webb and Fresco, 1973; Gartland and Sueoka, 1966; Streek and Zachau, 1971; Muench, 1969). While it is generally assumed that the native yeast $tRNA^{Leu}$ has the cloverleaf structure, the structure of the denatured conformer has been difficult to elucidate. In a recent note we presented the results of a preliminary investigation of the high-resolution nuclear magnetic resonance (nmr) of yeast $tRNA^{Leu}$ and proposed a model for the D conformer (Kearns *et al.*, 1974). In the present paper we report the results of a more extensive investigation of the nmr spectra of both the N and D conformers which lend further support to our proposed model and at the same time provide additional information about certain structural features of the N conformer.

* From the Department of Chemistry, University of California, Riverside, California 92502, and the Department of Biochemistry, Louisiana State University, Baton Rouge, Louisiana 70803. *Received July 15, 1974.* This investigation was supported in part by a biomedical sciences support Grant No. RR 07010-06 from the General Research Branch Division of Research Resources, Bureau of Health Professions Education and Manpower Training, National Institutes of Health, the U. S. Public Health Service (Grant GM 19313 to D.R.K.) and of the National Science Foundation (Grant GC 17124 to S.H.C.).

Experimental Section

(*a*) *Samples.* Pure $tRNA^{Leu}_3$ was prepared according to a procedure recently reported by one of us (Chang *et al.*, 1973a,b). A solution of yeast tRNA was heated at 60° for 5 min in the presence of 10 mM $MgCl_2$ and cooled 25°. This "heat activated" tRNA was then subjected to chromatography in two consecutive columns of BD-cellulose, first in the presence of magnesium ion and second in the absence of this cation. The partially purified $tRNA^{Leu}_3$ was specifically converted into its denatured form ($tRNA^{Leu}_3$ D) and finally purified in a column of Sephadex G-100. Based on [^{14}C]leucine acceptance and T_1 ribonuclease degradation, it was judged to be higher than 90% pure. The tRNA in 0.1 M KCl and cacodylate buffer (10^{-2} M, pH 7.0) was denatured by incubation with EDTA (10^{-2} M) at 60° for 5 min. The solution was concentrated by vacuum dialysis *vs.* the cacodylate buffer to 55 mg of tRNA/ml. After recording the nmr spectra of these denatured samples, the tRNA was directly renatured in the sample tube by adding KCl to 0.15 M and $MgCl_2$ to 0.01 M, and incubating for 2 hr at 40°. Quantitative renaturation was confirmed by assay of leucine acceptor activity.

(*b*) *Nmr Spectra.* Nmr spectra were obtained with a Varian Associates HR 300 nmr spectrometer operating at 300 MHz and were time averaged for 1–3 hr to improve signal-to-noise. Sample volumes were ~0.12 ml (Wilmad microcells), the tRNA concentration was ~55 mg/ml, and the temperature was controlled to ±1°. The nmr spectra of the native and denatured conformers at several different temperatures are presented in Figures 1 and 2. When the spectrum of the native conformer is subtracted from the spectrum of the denatured conformer the difference spectrum shown in Figure 3 is obtained.

Two different methods were used to determine the number of exchangeable protons per tRNA molecule in the low-

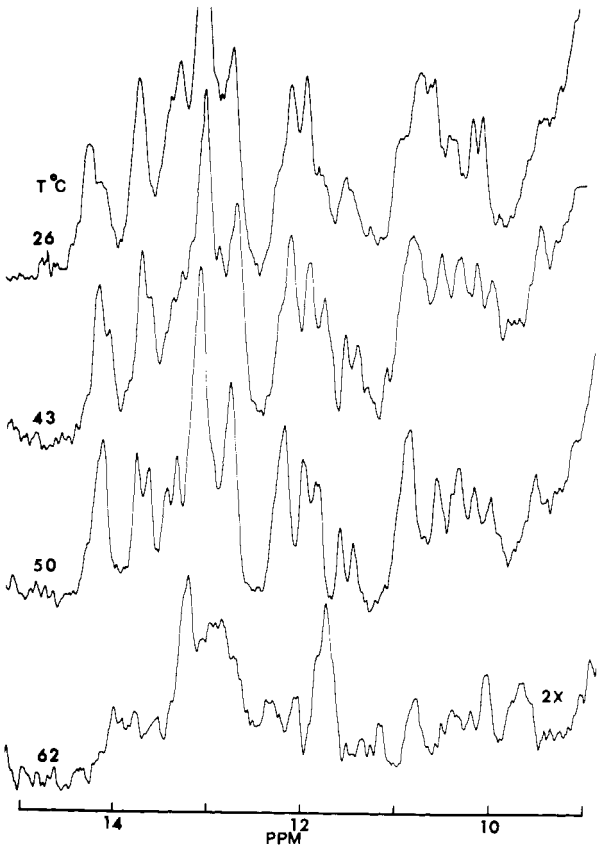

FIGURE 1: Temperature dependence of the 300-MHz proton nmr spectrum of the native conformer of yeast $tRNA^{Leu_3}$ in a solution containing 0.15 M KCl, 10 mM $MgCl_2$, and 10 mM cacodylate buffer at pH 7. The tRNA concentration was 55 mg/ml.

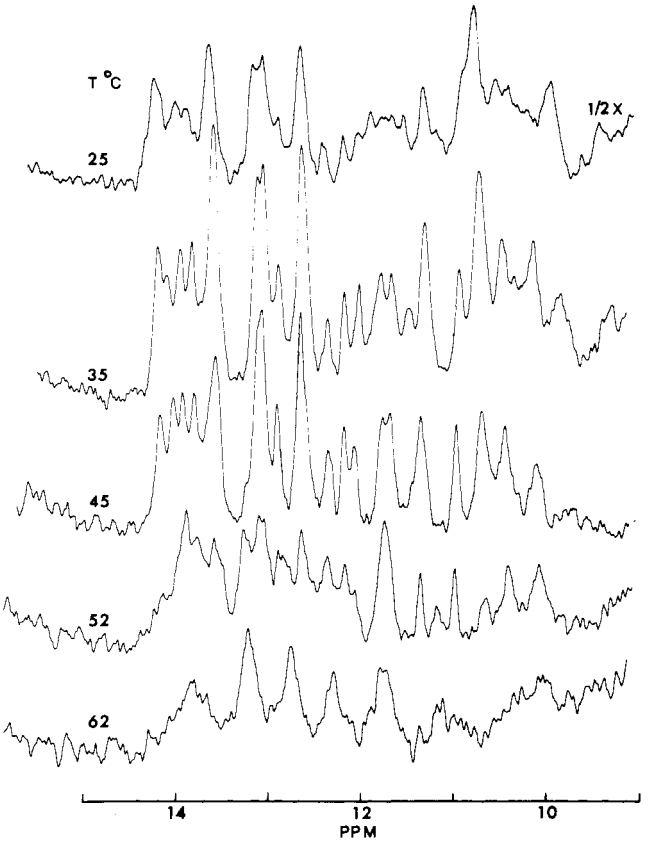

FIGURE 2: Temperature dependence of the 300-MHz proton nmr spectrum of the denatured conformer of yeast $tRNA^{Leu_3}$ in a solution containing 0.1 M KCl and 10 mM cacodylate buffer at pH 7. The tRNA concentration was 55 mg/ml.

field region. In the first method, the integrated intensity in the appropriate spectral region of the $tRNA^{Leu_3}$ sample (11–15 ppm and 9–11 ppm) was compared with the integrated intensity of a standard sample of $tRNA^{Phe}_{yeast}$ (1.4 mM) which exhibits 19 resonances in the 11–15-ppm region (Wong *et al.*, 1972). This led to a value of 21 ± 2 (Wong *et al.*, 1973). In the second method we assume that a separately resolved peak in the nmr spectrum of the native conformer ($tRNA^{Leu_3}$ N) corresponds to an integral number of protons/molecule and then used this to integrate (Wong *et al.*, 1973). In the case of $tRNA^{Leu_3}$ N the peak at 14.3 ppm was assumed to correspond to two protons and the rest of the spectrum was integrated on this basis and these results are shown in Figure 4. This method also gave a value of 21 ± 2 base pairs for the native conformer at 26°. Since measurements were made on the same sample in the same nmr tube before renaturing, this also provided a basis for integrating the spectrum of the denatured leucine. Based on this number the denatured conformer contains three less base pairs, or a total of 18 ± 2 base pairs at 25 or 35° (Wong *et al.*, 1973). With the specific salt conditions listed in Figures 1 and 2, we found that the melting and cooling of the samples was perfectly reversible. Each sample returned to its original low-temperature form after cooling to room temperature without any interconversion between the two forms. Addition of Mg^{2+} to the denatured conformer produced no change (for at least 2 hr) in the spectrum until the sample was heated.

(*c*) *Optical Studies.* Optical measurements were carried out using tRNA solutions having an absorbance of about 1.0 at 260 nm. The melting curves were obtained with a rapid heating and cooling device developed in this laboratory (Rordorf) which required only 5–10 min for a complete heat-cool cycle. The results of these measurements are shown in Figure 5.

(*d*) *Base Pairing Matrix Map and Pairing Schemes.* To investigate the possible base-pairings schemes for yeast $tRNA^{Leu}$ (see Figure 6 for sequence) we have determined

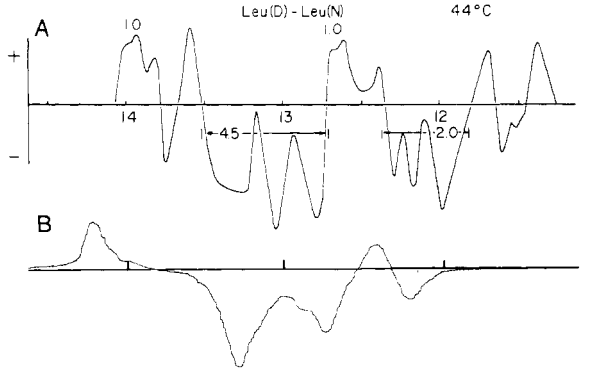

FIGURE 3: (A) The 300-MHz proton nmr D–N difference spectrum obtained by subtracting the spectrum of the native conformer from the spectrum of the denatured conformer of yeast $tRNA^{Leu_3}$ (temperature, 44°). The approximate integrated intensities (protons/molecule) are also shown for various spectral regions. (B) The D–N difference spectrum computed on the assumption that the N conformer has the cloverleaf structure and the D conformer has the structure shown in Figure 9. For the purposes of these calculations it was also assumed that the amino acid acceptor stem and the TψC stem are stacked in both the N and the D conformers. The lowest field peak in the computed D–N spectrum corresponds to one proton/molecule.

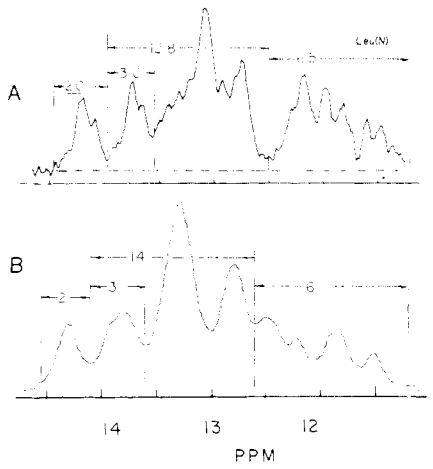

FIGURE 4: A comparison of the observed low-field nmr spectrum of the N conformer (A) at 44° with that predicted for the cloverleaf model (B). In the observed spectrum, the peak centered at 14.2 ppm was assumed to correspond to 2 protons/molecule and the rest of the spectrum was integrated using this reference. The base line used in the integration is shown by the dashed line. The intensity in corresponding regions of the computed spectrum are also indicated for comparison.

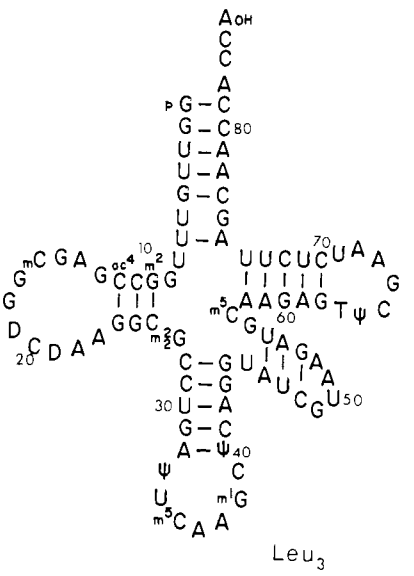

FIGURE 6: The sequence of yeast $tRNA^{Leu}_3$ shown in the cloverleaf form (Chang *et al.*, 1973).

all possible continuous helices containing three or more base pairs, and these are listed in Table I. Many of these helices are mutually exclusive of one another and this has been indicated in the compatibility matrices shown in Table V and Table VIII in the Appendix for two particular sets of helices which were found to be important to our analysis. From this information, allowed pairing schemes for the entire molecule can be constructed.

(*e*) *Computation of the Nmr Spectra of Individual Helical Stems.* On the basis of earlier studies the following interpretation can be given to the tRNA nmr spectra (Kearns *et al.*, 1973; Lightfoot *et al.*, 1973; Shulman *et al.*, 1973a,b). The hydrogen bonded ring nitrogen proton from each Watson–Crick base pair (AU, Aψ, or GC) contributes *one* and only one resonance to the low-field nmr spectrum in the region between 11 and 15 ppm. In the double helix resonances from the AU (Aψ) and GC base pairs are upfield shifted from their intrinsic (unshifted) positions by ring current fields generated by neighboring bases, and Table II lists a set of parameters which give a satisfactory account of the spectrum of a number of other tRNA species, tRNA fragments, and model compounds (Lightfoot *et al.*, 1973; Kearns and Shulman, 1974). These values, when combined with the intrinsic AU and GC positions (AU^0 = 14.5 ppm, GC^0 = 13.6 ppm, and Aψ = 13.5 ppm), permitted us to compute the low-field nmr spectra expected for all helices listed in Table I. These were combined to generate spectra for different pairing schemes.

In earlier work we used slightly different parameters for the intrinsic positions (*e.g.*, AU^0 = 14.8, GC^0 = 13.7 ppm) and correspondingly had to use slightly larger (by about 20%) values for the nearest neighbor ring current shifts than those used here (Lightfoot *et al.*, 1973; Shulman *et al.*, 1973a). Based on more recent work (Wong and Kearns, 1974; Rordorf, unpublished results; Jones, unpublished results) this small revision of the original paramaterization seems desirable.

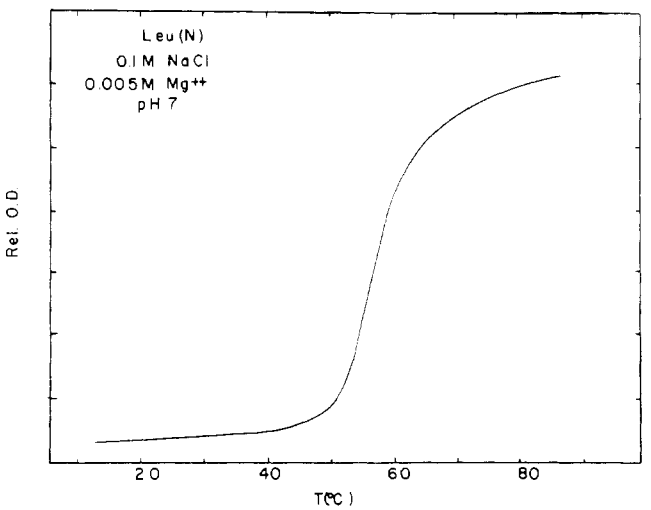

FIGURE 5: Optical melting behavior of yeast $tRNA^{Leu}_3$ in a solution containing 5 mM $MgCl_2$, 10 mM cacodylate (pH 7), and 0.1 M NaCl.

Results and Discussion

(*a*) *Analysis of the Nmr Spectrum of the N Conformer.* Integration of the low-field nmr spectrum of the N conformer indicates that it contains 21 ± 2 base pairs (Wong *et al.*, 1973). The *total* number of base pairs is consistent with the number required by the cloverleaf model and the nmr spectrum computed for this model is in good agreement with the observed spectrum as the results shown in Figure 4 and Table III indicate. Not only is there good agreement between the computed and observed total number of base pairs, but the relative intensity in the different portions of the spectrum is well accounted for by the computed spectrum. Although most of the peaks in the computed spectrum are shifted by 0.1–0.2 ppm to lower field relative to those in the observed spectrum this discrepancy is within the expected accuracy of the calculations, and could actually be removed if we shifted the intrinsic positions of AU and GC by 0.1–0.2 ppm.

In computing the spectrum it was necessary to make assumptions regarding the stacking of bases adjacent to the terminal base pairs of each helical stem. In the results shown in Figure 4B we assumed stacking of the TψC and the amino acid acceptor stems to form a single continuous helix, stacking of G_{56} on AU_{46} of the minor stem, and stacking of G_{13} on GC_{12}. If these stacking interactions are

TABLE I: A List of All Possible Helices for Yeast $tRNA^{Leu}_3$.

Helix No.	Paired Bases	No. of Base Pairs	Comments
H_1	4–7, 14–16		Unstable, 3 base pairs with 1 GU pair.
H_2	11–13, 16–18		Unstable, short loop
H_3	10–12, 24–26	3	DHU stem
H_4	15–17, 26–28	3	
H_5	9–11, 27–29	3	
H_6	23–25, 28–30		Unstable, short loop
H_7	30–32, 34–36		Unstable, short loop
H_8	3–5, 35–37	3	
H_9	7–9, 35–37	3	
H_{10}	13–15, 39–41	3	
H_{11}	28–32, 40–44	5	Anticodon stem
H_{12}	31–33, 46–48	3	
H_{13}	12–14, 47–49	3	
H_{14}	46–48, 53–55	3	Minor stem
H_{15}	3–5, 57–59	3	
H_{16}	7–9, 57–59	3	
H_{17}	32–35, 60–63	3	
H_{18}	39–41, 60–62	3	
H_{19}	12–16, 62–66	4	
H_{20}	6–9, 65–68	3	
H_{21}	47–49, 65–67	3	
H_{22}	31–35, 66–70	5	
H_{23}	63–65, 66–68		Unstable, short loop
H_{24}	1–4, 67–70	3	
H_{25}	42–45, 68–71	3	
H_{26}	52–55, 68–71	4	
H_{27}	59–61, 69–71	3	
H_{28}	13–15, 70–72	3	
H_{29}	58–62, 70–74	5	TψC stem
H_{30}	50–54, 71–75	5	
H_{31}	22–24, 72–74	3	
H_{32}	29–32, 73–76	3	
H_{33}	1–7, 75–81	6	Amino acid stem
H_{34}	55–57, 76–78	3	
H_{35}	7–9, 77–79	3	
H_{36}	5–7, 78–80	3	
H_{37}	62–64, 78–80	3	
H_{38}	43–45, 79–81	3	
H_{39}	7–10, 80–82	3	
H_{40}	1–3, 82–84	3	
H_{41}	43–45, 82–84	3	
H_{42}	8–10, 83–85	3	

TABLE II: A Summary of the Ring Current Shift Parameters and Intrinsic Positions (in ppm) Used in Calculating the Positions of the Low-Field Proton Resonances for AU or GC Base Pairs.[a]

Sequence	Ring Current Shift of the AU Proton Due to Bases X and Y			
	X Base	Shift	Y Base	Shift
5′ | – | 3′	A	1.1	U	0.1
– |	G	0.6	C	0.2
–X	C	0.1	G	0.6
U–A	U	0	A	0.6
Y– |				
– |				
3′ | 5′				

Sequence	Ring Current Shift on GC Proton Due to Bases X and Y			
	X Base	Shift	Y Base	Shift
5′ | – | 3′	A	1.1	U	0.1
– |	G	0.7	C	0.25
– |	C	0.2	G	0.7
–X	U	0.1	A	1.0
C–G				
Y– |				
– |				
– | 5′				
– |				
3′ |				

[a] The unshifted positions for the base pairs are: $(AU)^0$ = 14.5 ppm, $(GC)^0$ = 13.6 ppm.

not present, then the resonance from AU_{46} shifts from 13.9 to 14.5 ppm and there is a loss of intensity in the 13.2-ppm region of the spectrum. Since both of these changes lead to poorer agreement between the computed and observed spectra we conclude that the original assumptions were valid.

It is gratifying to see a good fit of the spectrum in the region between 14.5 and 12 ppm. We are less concerned about the fit in the region between 11 and 12 ppm for two reasons. First of all, resonances in this region have been greatly shifted from their intrinsic position and hence are very sensitive to very small deviations from the assumed perfect helical geometry. Secondly, some resonances in the 11.0–11.5-ppm region may be due to G or U ring nitrogen protons which are not in base pairs, but are protected from rapid exchange with the water (Wong and Kearns, 1974).

On the basis of the good agreement between the experimental spectrum, and that computed for the cloverleaf model, some resonances can be assigned to specific base pairs. The two lowest field resonances at ~14.2 ppm can be assigned to AU_3 in the amino acid acceptor stem and AU_{47} in the minor loop stem. Similarly, the peak at 13.8 ppm corresponding to about three protons can be attributed to AU_{46} from the minor stem and AU_{59} and AU_{31} from the TψC stem. Possible assignments of other resonances are indicated in Table III. Since the cloverleaf model permits a good fit of the nmr spectrum, other possible pairing schemes can be judged relative to this model, and these are discussed in the Appendix. As we show there, no other model which retains the amino acid acceptor stem gives as good account of the nmr. Therefore, based on the nmr data, the cloverleaf model is the most reasonable structure for the N conformer.

(*b*) *Temperature Dependence of the Native $tRNA^{Leu}$ Low-Field Nmr Spectra.* The temperature dependence of the nmr spectrum of $tRNA^{Leu}_N$ is shown in Figure 1. To emphasize the temperature dependent features in the spectrum the 26 and 50° spectra are shown superimposed in Figure 7. This comparison shows that there is a loss of intensity at 13.8 (one proton), 13.3 (1.5 proton), 12.8 (~0.8 proton), 12.0 (1.1 proton), 11.8 (1 proton), and 11.4 (~0.5 proton). Most of these changes can be accounted for in terms of the loss of the DHU stem along with the reso-

TABLE III: A Summary of the Assignments of the Low-Field Resonances of the Native Conformer of Yeast $tRNA^{Leu}_3$.

Resonance Intensity[a]	Location (ppm)	Assignment[b]	Calculated Position
2	14.3–14.2	AU_{47}	14.3
		AU_3	14.3
		AU_{40}	13.9
~3	13.7	AU_{59}	13.8
		AU_{63}	13.7
		GC_{62}	13.4
		GC_2	13.3
		GC_{28}	13.3
6–7	13.4–12.8	AU_{30}	13.3
		$A\psi_{32}$	13.3
		GC_{11}	13.2
		AU_7	13.2–13.9[c]
		AU_{58}	12.8–13.5[c]
		GC_{29}	12.8
~3	12.7	AU_4	12.8
		GC_{10}	12.7
		GC_5	12.5
		GC_{60}	12.4
		GC_{12}	12.2
~7	12.4–11.3	GC_1	11.9
		GC_{48}	11.8
21.3		GC_{31}	11.5

[a] Protons per molecule. [b] Unshifted positions: AU = 14.5, GC = 13.6, Aψ = 13.5 ppm. [c] Exact location depends upon orientation of amino acid acceptor stem relative to the TψC stem.

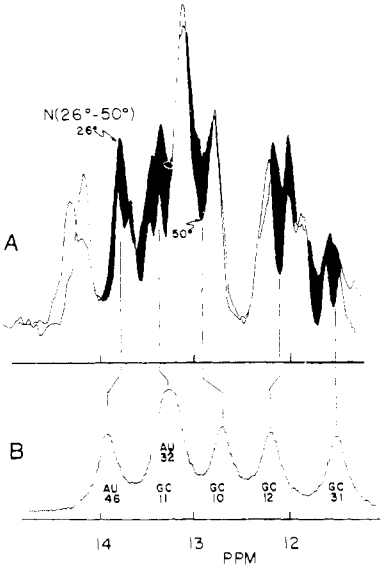

FIGURE 7: (A) A comparison of the 300-MHz proton nmr spectrum of yeast $tRNA^{Leu}_3$ at 26 and 50°. The differences between the two spectra have been darkened to emphasize the loss in intensity that has occurred at 50°. (B) Calculated difference spectrum assuming loss of the DHU stem (base pairs GC_{10}, GC_{11}, and GC_{12}), the terminal base pairs $A\psi_{32}$ and AU_{46}, and the resonance from GC_{31} adjacent to $A\psi_{32}$.

nances from the terminal $A\psi_{32}$ and AU_{46} base pairs, and GC_{31} adjacent to $A\psi_{32}$. The loss of intensity in the 13.3-ppm region is attributed to the loss of $A\psi_{32}$ since this resonance is predicted to be at 13.3 ppm and we already know from studies of other tRNA fragments (Kearns *et al.*, 1973; Lightfoot *et al.*, 1973; Wong and Kearns, 1974) that terminal Aψ base pairs are particularly susceptible to early melting. Loss of the DHU stem accounts for the remainder of the intensity loss observed at 13.2, 12.8, and 12.0 ppm. The 13.8-ppm resonance probably represents the loss of the terminal AU_{46} base pair from the minor stem (predicted at 13.9 ppm). As noted above, resonances in the 11.5–11.0-ppm region are not well understood and there is a lot of intensity in this particular tRNA in the 11.0–10.0-ppm region which is yet to be properly assigned. Thus, while some loss of intensity in the 11.5-ppm region could be due to loss of an extra resonance from a protected G or U residue, it might be due to broadening of GC_{31} accompanying the loss of the adjacent $A\psi_{32}$ base pair.

By 62° there are significant losses of intensity throughout the 11.0–15.0-ppm region. Examination of the predicted positions of the resonances associated with various stems of the cloverleaf indicates that the 62° spectrum can best be accounted for in terms of resonances from the anticodon stem and the amino acid acceptor stem. At this elevated temperature the terminal AU_7 and $A\psi_{32}$ will undoubtedly be absent and even resonances from internal AU base pairs may be broadening at this point.

This interpretation of the 62° spectra is consistent with the fact that the amino acid stem and the anticodon stems are expected to be the most stable ones (Tinoco *et al.*, 1971; Gralla and Crothers, 1973). It also fits with the observation that the two broad resonances in the spectrum (located around 12.0 and 14.0 ppm) are both assigned to AU base pairs (AU_3, AU_4) whereas the sharp resonances at 11.8 and 13.2 ppm are assigned to GC base pairs ($GC_{1,2}$). The fact that the sequential loss of resonances from this molecule can be accounted for in terms of the cloverleaf model provides additional support for the correctness of this model.

It is interesting to note that the optical melting data shown in Figure 5 provide little or no indication for multiphasic melting under similar experimental conditions. This, in part, is due to the fact that loss of resonances in the nmr spectrum corresponds to an earlier stage in the disruption of a double helix and to the fact that single- as well as double-stranded regions of the molecule contribute to the optical melting phenomenon (Reisner and Römer, 1973; Crothers *et al.*, 1973).

While there is substantial evidence supporting many general features of the cloverleaf model (Henley *et al.*, 1966; Fresco *et al.*, 1966; Lindahl *et al.*, 1966, 1967; Uhlenbeck *et al.*, 1972; Webb and Fesco, 1973; Gartland and Sueoka, 1966), the nmr data, and the analysis of the spectra presented here provide the most detailed experimental support for the number and types of base pairs required by the model. In addition, these results also provide some tertiary structural information.

(*c*) *Denatured Conformer of $tRNA^{Leu}_3$.* The spectrum of the denatured form of $tRNA^{Leu}_3$ (Figure 2) is rather remarkable in that it is extremely well resolved. While part of the resolution may be attributed to the high AU content of $tRNA^{Leu}$, this cannot be the entire reason since yeast $tRNA^{Phe}$ has a similar AU/GC composition.

Integration of the nmr spectrum of the D conformer indicates that it contains a total of 18 ± 2 base pairs, and an accurate comparison of the spectra of the two conformers indicates that the D conformer contains a total of three less base pairs than the N conformer (Wong *et al.*, 1973). The difference spectrum shown in Figure 3 further indicates

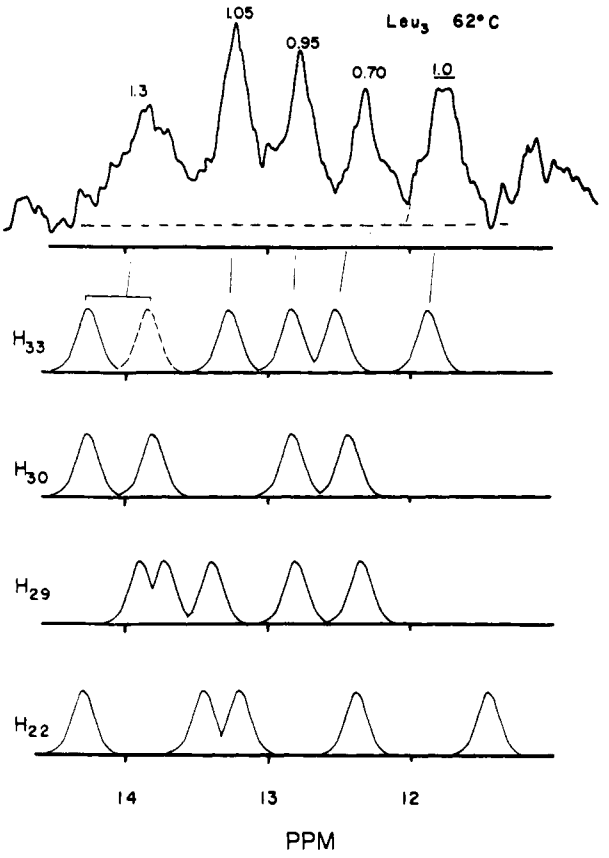

FIGURE 8: A comparison of the 62° spectrum of the D conformer with the spectrum predicted for the amino acid acceptor stem (H_{33}) and other possible helices. The observed spectrum is shown at the top of the figure along with the integrated intensities of each peak (relative to the peak at 11.8 ppm which is taken as 1.0). The assumed base line is shown as a dashed line. The terminal AU_7 peak in the spectrum for H_{33} is shown as a dashed peak because it is expected to be missing from the high-temperature spectrum.

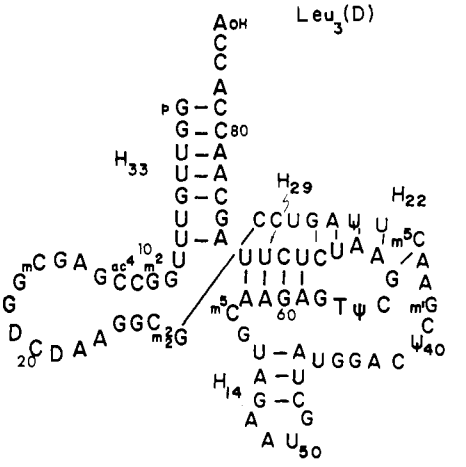

FIGURE 9: Proposed model for the secondary structure of the denatured conformer of yeast tRNA^{Leu_3}.

that the net loss of three base pairs is due to a loss of at least five of the original base pairs and a gain of at least two new base pairs. The nmr spectra clearly indicate that there are rather substantial differences between the secondary structures of the native and denatured conformers and, rather surprisingly, that the denatured conformer is more stable than the native conformer in the magnesium free, low salt solutions, despite the fact that the native conformer contains more base pairs.

The analysis of the D conformer nmr spectrum is simplified by considering the 62° spectrum first (Figure 8). At this temperature the total intensity remaining in the nmr spectrum corresponds to approximately 5–6 protons per molecule and 5 distinct peaks are observed. By comparison with the lower temperature spectra (Figure 2) it may be seen that the lowest field resonance at 13.8 ppm is probably associated with a peak which starts out at 14.2 ppm at 25° and progressively shifts upfield upon heating. The other resonances observed in the 63° spectrum appear to be little shifted from their positions observed in the lower temperature spectrum.

Examination of the set of nmr spectra predicted for each of the possible helices listed in Table I indicates that the only helices which have the proper number and spectral distribution of resonances are H_{22}, H_{29}, H_{30}, and H_{33}. Of this set, H_{33}, the amino acid acceptor stem, is the only one which satisfactorily accounts for the observed resonances as the comparison between the observed and predicted spectrum shown in Figure 8 indicates. The terminal AU_7 base pair (predicted position = 13.9 if TψC stem melted) may very well be missing from the high-temperature spectrum and is therefore shown as a dashed curve. The other three helices (H_{22}, H_{29}, and H_{30}) all give incorrect intensity distributions (as seen in Figure 8).

As noted above, the 13.8-ppm resonance in the 62° spectrum is due to a resonance which has shifted upfield by 0.4 ppm from its position at 14.2 ppm in the low-temperature spectrum. An entirely similar temperature sensitive resonance was observed in the N conformer, and in both cases the resonance is assigned to AU_3 of the amino acid acceptor stem. Taking these factors into consideration, we conclude that the amino acid acceptor stem is the only one which is present at 62° and this information may now be used in analyzing the low-temperature spectrum.

To accomplish this, we constructed all possible pairing schemes which contained the amino acid acceptor stem, and a total of approximately ~18 base pairs. We introduced the further stipulation that the predicted spectrum for any model had to account for the room temperature spectrum of the D conformer and for the D–N difference spectrum. Finally, we made use of the oligonucleotide binding data of Uhlenbeck and Fresco (Uhlenbeck *et al.*, 1972) which indicate that the DHU loop and stem regions must be single stranded in the D conformer. The only two pairing schemes consistent with all of these requirements are

Scheme I: [H_{33} + H_{29} + H_{22} + H_{14}]

Scheme II: [H_{33} + H_{30} + (H_{12} or H_{17}) + H_{41}]

Of the two, we favor Scheme I which retains the minor stem, the TψC stem, and the amino acid acceptor stem from the N conformer, but replaces the anticodon stem with H_{22}. This model is shown in Figure 9 and the nmr spectrum predicted on the basis of this model is shown in Figure 10 and in Table IV. As with the N conformer, we assumed stacking of the amino acid acceptor stem and the TψC stem. If these two stems are not stacked a poorer fit of the spectrum is obtained. In Figure 10 we have also shown the computed and observed integrated intensities in various spectral regions. In general the agreement between the computed and observed results is good and even better correspondence would be obtained if the computed spectrum were displaced upfield by 0.1–0.2 ppm. In the computed spectrum there does appear to be too much intensity at 12.5 ppm and too little

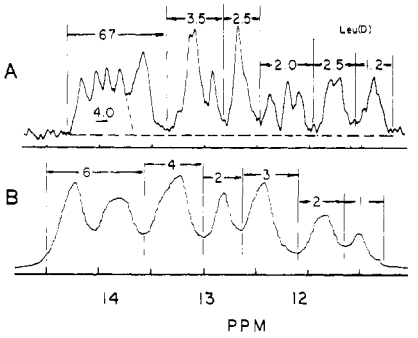

FIGURE 10: A comparison of the low-field nmr spectrum of the D conformer of $tRNA^{Leu}_3$ (temperature, 44°) with that predicted for the model shown in Figure 9. The observed spectrum (A) was integrated by assuming that the collection of four low-field peaks correspond to 4 protons/molecule and the intensities in various regions of the spectrum are shown in (A). The base line used in the integration is given by the dashed line. Comparison of the total intensity obtained by this method agrees with the total intensity obtained by comparing the N and D conformer spectra. This integrated intensity in various regions of the computed spectrum (B) is shown for comparison.

intensity at 12.8 ppm and it is interesting to note that $G_{31}C_{70}$ is contributing one of the resonances to 12.5 ppm. Because of its location at the terminus of helix H_{22} this base pair may be susceptible to "end effects" (Wong and Kearns, 1974; Rordorf, unpublished results) which could displace it from 12.5 ppm.

The calculated difference between the spectrum of the D and the N conformer based on the model shown in Figure 9 for the D conformer and the cloverleaf model for the N conformer is shown in Figure 3 along with the observed difference spectrum. Within the expected accuracy of the method (usually 0.1–0.2 ppm) the computed spectrum generally accounts for observed D–N difference spectrum. In particular, the gain of intensity around 14.0 ppm (calcd 14.2 ppm) and 12.6 ppm (calcd 12.4 ppm) and the substantial loss of intensity between 13.5 and 12.7 ppm (calcd 13.4–12.5 ppm) are well accounted for. A small shift of the resonance from terminal base pair $A_{59}U_{73}$ or $A_{61}U_{71}$ is all that would be required to improve the fit in the 13.5–13.8-ppm region. With the exception of Scheme II, no other pairing scheme could account for the major features in the D–N difference spectrum, nor give as good a fit of the D conformer spectrum.

Scheme II is less desirable than the model shown in Figure 9 since it leaves bases in the anticodon loop unpaired if H_{12} is used (but not if H_{17} is used), does not provide a good account of the melting behavior of the D conformer (see discussion below), and involves the formation of a rather weak helix containing only two AU and one GC pair. These factors taken collectively argue against this pairing scheme. Experimentally, it would be possible to rigorously distinguish between these two models by removing the ACCA 3′ terminus of the molecule since this would eliminate the possibility of forming H_{41} which is needed in Scheme II.

Other pairing schemes which can be constructed for the D conformer are discussed in the Appendix. None were as successful in accounting for the observed spectra and are therefore not considered further here.

(*d*) *Temperature Dependence of the Low-Field Nmr Spectrum of the Denatured Conformer of* $tRNA^{Leu}_3$. We mentioned earlier in connection with the analysis of the N conformer that the temperature dependence of the nmr spectrum provides an additional way of testing our proposed model. The temperature dependence of the $tRNA^{Leu}$ D

TABLE IV: A Summary of the Assignments of the Low-Field Resonances of the Denatured Conformer of Yeast $tRNA^{Leu}_3$ Based on the Model Shown in Figure 9.

Resonance Intensity[a]	Location (ppm)	Assignment[b]	Calculated Position (ppm)
1	14.25	A_{79} U_3	14.3
1	14.1	A_{32} U_{69}	14.3
1	14.0	A_{54} U_{47}	14.3
1	13.8	A_{46} U_{55}	13.9
2.7	13.7	A_{59} U_{73}	13.8
		A_{61} U_{71}	13.7
		A_{68} ψ_{33}	13.4
3.5	13.2–12.8	G_2 C_{80}	13.3
		A_{67} U_{34}	13.2
		A_{75} U_7	13.2–13.8[c]
2.5	12.6	A_{58} U_{74}	12.8–13.4[c]
		A_{78} U_4	12.8
2	12.4–12.0	G_5 C_{77}	12.5
		G_{60} C_{72}	12.4
		G_{31} C_{70}	12.4
2.5	11.8	G_1 C_{81}	11.9
		G_{53} C_{48}	11.8
1.2	11.4	$G_{66}m^5C_{35}$	11.5
18.2			

[a] Protons per molecule. [b] Based on model shown in Figure 9. [c] Sensitive to relative orientation of amino acid acceptor stem and TψC stem.

spectrum is shown in Figure 2 and it is evident from these data that the loss of resonances occurs sequentially rather than cooperatively. Under the conditions used in these experiments the D form is not converted to the N form since heating and cooling are perfectly reversible. This indicates that under the salt conditions used in our experiments the D form is the thermodynamically stable form. Conversion to the N form requires not only the addition of higher salt, but also magnesium ion.

Comparison of the 25 and 45° spectra indicates a slight loss of intensity at 13.5 ppm and by 52° there are rather substantial losses in intensity. The comparison of the 35 and 55° spectra shown in Figure 11 graphically illustrates the changes which occur over this temperature range. Integration of the spectrum indicates a loss of approximately nine resonances at 52°. In Figure 11A,B the observed intensity losses are compared with those which would be predicted for the loss of the minor stem (H_{14}) and the helix (H_{22}) which is unique to the denatured conformer. According to the model these two short helices are expected to be the least stable ones and we find that their predicted nmr spectra agrees reasonably well with the set of resonances lost when the sample is heated to 52°. A slightly better fit of the loss spectrum is obtained if the calculated spectrum is displaced upfield by about 0.2 ppm. Heating the D conformer from 52 to 62° results in a further reduction in intensity corresponding to a loss of ~4 more resonances. Comparison of the loss spectrum (see Figure 11C,D) with the nmr spectrum predicted for the TψC stem (which contains only four base pairs in the model) shows that there is good agreement. The sequential melting of the D conformer involves

then first the loss of the minor stem (H_{14}) and the new stem (H_{22}) followed by the TψC stem (H_{29}). The amino acid acceptor stem (H_{33}) remains to the last and the 62° spectrum (shown in Figure 8) is well accounted for in terms of the base pairs in the amino acid acceptor stem (recall AU_3 shifts with temperature).

The fact we can give a reasonably good account of the temperature dependence of the D conformer provides an additional piece of evidence supporting our proposed model.

(*e*) *Relation of the D Conformer Structure to Other Experimental Results.* There is a good deal of information on the physical properties of the N and D conformers of yeast $tRNA^{Leu}_3$ available from other types of measurements and it is interesting to compare and contrast these with our nmr results. One important observation is that there is an activation energy of 68 kcal associated with the conversion of the D to the N conformer (Webb and Fresco, 1973), and on this basis it was concluded that some new base pairs in the D form have to be broken before the N conformer can be formed. Our earlier nmr observations confirmed that this is the case (Wong *et al.*, 1973) and the results presented here have now provided detailed information on the base pairing changes which occur on conversion from the D to the N conformer. According to our interpretation of the nmr spectrum of the D conformer, helix H_{22}, which contains 4–5 base pairs, must be broken in order to reform the N conformer. Since the ΔH per base pair is of the order of 10 kcal our model would predict a ΔH of 40–50 kcal for the D–N conversion.

Although we built in the requirement that the dihydro loop and stem region be single stranded in the D conformer, it is interesting to note that bases 33–35 from the anticodon loop are paired in our model. On the other hand, bases 40–45 which are paired in the N conformer are single stranded in the D conformer, and therefore perhaps susceptible to chemical reaction and/or enzymatic cleavage. These features fit well with the observations of Uhlenbeck *et al.* (1972) which indicate that the anticodon loop is protected in the D conformer. They also allow specific predictions to be made which would differentiate between our model and all other models which retain the anticodon stem.

The initial optical studies indicated no significant difference in the *total* number of base pairs in the N and D forms, although there were suggestions that N forms contained more AU pairs than the D form (Fresco *et al.*, 1966; Lindahl *et al.*, 1966). CD experiments revealed only marginal differences (within experimental error perhaps the same). Tritium exchange experiments and the centrifugation measurements indicate that the D conformer has a more open structure relative to the N structure and this too is in agreement with our model (as well as others) (Webb and Fresco, 1973).

Finally, as we have noted, the D conformer acts as a competitive inhibitor of the charging of the N conformer, indicating that it contains some features of the original cloverleaf model. This too is reasonable in terms of our model which retains three of the helices originally present in the cloverleaf model.

Summary

In this paper we have described the way in which an analysis of high-resolution nmr spectra may be used to deduce information about the secondary structure of a tRNA molecule in solution. We find that the base pairing in the native conformer of yeast $tRNA^{Leu}_3$ is perfectly consistent with the cloverleaf model and that other possible base-pairing schemes give poorer fits of the nmr spectrum. Some individual resonances in the low-field nmr spectra can be assigned to specific base pairs in the cloverleaf, and these should be useful for future structural and metal binding studies. The temperature dependence of the low-field nmr spectrum demonstrates that the loss of resonances from the spectrum of the native conformer is not nearly so cooperative as indicated by optical measurements carried out under similar conditions. From an analysis of the nmr spectra we conclude that resonances from the DHU stem are lost first whereas resonances from the amino acid acceptor stem are among the last to be lost.

Analysis of the nmr spectrum of the D conformer leads to a model in which the DHU stem and the anticodon stem of the cloverleaf are replaced by a single helix involving pairing of bases in the anticodon loop with bases in the TψC loop. Alternative schemes do not give nearly as good an account of the nmr data. Another model which retains only the amino acid acceptor stem of the cloverleaf cannot be rigorously excluded by the nmr data, but for various reasons is less satisfactory.

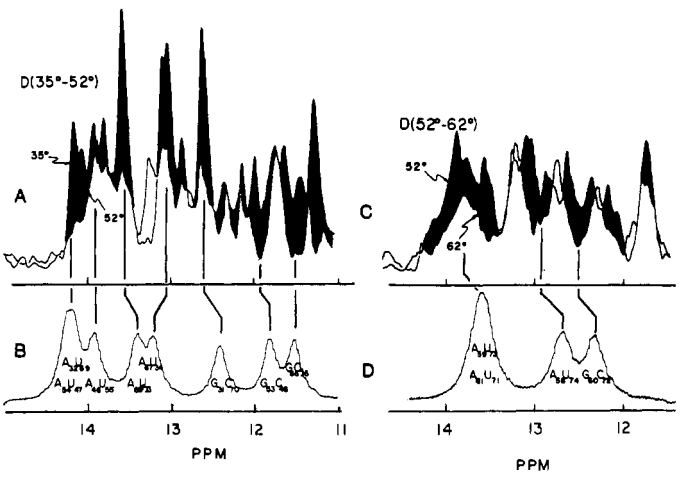

FIGURE 11: (A) Comparison of the spectrum of the D conformer at 35 and 52°. (B) Predicted difference spectrum assuming the loss of the minor stem (H_{14}) and H_{22} from the model shown in Figure 9. (C) Comparison of the spectrum of the D conformer at 52 and 62°. (D) Predicted difference spectrum assuming the loss of the TψC stem. The position of $A_{58}U_{74}$ is uncertain due to end effects.

Acknowledgments

We thank Mr. F. Rordorf for measuring the optical melting curves, Mr. T. Early for carrying out the computer analysis, and Mr. Frank Bosco of Wilmad Glass Company for his aid.

Appendix

1. Analysis of the Nmr Spectrum of the N Conformer. If there are no initial restrictions, then an enormous number of different pairing schemes can be constructed for $tRNA^{Leu}_3$. However, if we make use of experimental information already available, then the number of possibilities is greatly reduced. One feature which is common to all tRNA molecules and which appears to be required is the amino acid acceptor stem. The oligonucleotide binding data of Uhlenbeck *et al.* (1972) clearly indicate that the DHU loop and the anticodon loop regions are single stranded and we have accordingly included both of these features in our search for possible base-pairing schemes for the N confor-

TABLE V: A Matrix Illustrating the Compatibility of Helices Which Could be Present in a Structure Which Contains the Amino Acid Acceptor Stem (H_{33}) but no Base Pairs Involving Bases in the DHU Loop or the Anticodon Loop.[a]

	3	5	11	14	18	21	25	26	27	29	30
3		X									
5	X		X								
11		X			X		X				
14						X		X			
18			X				X		X	X	
21				X							
25			X		X			X	X	X	X
26				X			X		X	X	X
27					X		X	X		X	X
29					X		X	X	X		X
30				X			X	X	X	X	

[a] Incompatibilities are indicated by an X.

mer. Only a few helices are found consistent with these initial restrictions, and these are listed in Table V in the form of a compatibility matrix. Because of the fact that the helices H_{25}, H_{26}, H_{27}, H_{29}, and H_{30} are mutually exclusive the number of possible pairing schemes is limited to the set shown in Table VI. The nmr spectra computed for these eight schemes are presented in Figure 12.

The cloverleaf model (Model N_1) has already been discussed and shown to provide a good account of the nmr spectrum of the N conformer.

Model N_2 differs slightly from the cloverleaf in that the TψC stem is replaced by a very similar helix containing two less base pairs, and it correspondingly provides a less good fit of the spectrum, particularly in the region around 13.8 ppm.

Model N_3 has the right number of base pairs (21) and gives a very good account of the observed nmr spectrum. However, in this structure the minor stem and the TψC stem have been replaced by two other helices (H_{21} and H_{26}) which involve rather contorted base pairings. This fact, the fact that these two helices collectively have less GC content and overall one less base pair than minor stem and TψC stem, strongly suggests that this structure will be less stable than N_1, the cloverleaf. N_4 contains only 20 base pairs

TABLE VI: Possible Pairing Schemes for the Native Conformer of Yeast $tRNA^{Leu_3}$.[a]

Scheme Designation	Helices Present	Total No. of Base Pairs
N_1	3 + 11 + 14 + 29 + 33	22
N_2	3 + 11 + 14 + 27 + 33	20
N_3	3 + 11 + 21 + 26 + 33	21
N_4	3 + 11 + 21 + 27 + 33	20
N_5	3 + 11 + 21 + 29 + 33	22
N_6	3 + 11 + 21 + 30 + 33	21
N_7	5 + 18 + 21 + 29 + 33	20
N_8	5 + 18 + 21 + 30 + 33	19

[a] The base pairs present in the different helices listed in this table are indicated in Table I.

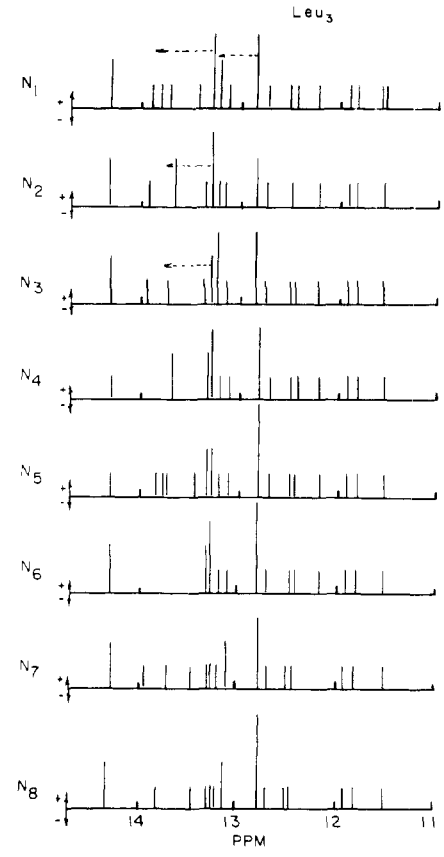

FIGURE 12: The predicted low-field nmr spectra for the set of eight possible native conformer structures listed in Table VI. The smallest vertical bars represent one resonance/molecule. The positions of some resonances are sensitive to stacking of helices and this has been indicated by arrows.

(within experimental error of the observed value), gives a poor account of the low-field region of the spectrum (14.3–13.7 ppm), and involves bonding between bases of the minor stem region and TψC loop region. N_5 differs from the cloverleaf only in that the minor stem (H_{14}) is replaced by H_{21} but this produces a more contorted structure and a poorer fit of the spectrum at 14.3 ppm. N_6 gives quite a poor fit of the spectrum in the 13.8-ppm region, and N_7 and N_8 contain only 19 or 20 base pairs, retain only one or two of the helices present in the original cloverleaf model, and actually do not give as good a fit of the spectrum as the cloverleaf model.

Therefore, subject to the minimal initial conditions stated, the cloverleaf model provides the best fit of the spectrum.

2. Analysis of the Nmr Spectrum of the D Conformer. In addition to the two models discussed in the text there are only a limited number of other possible models which retain the amino acid acceptor stem and which leave the DHU loop and stem regions single stranded. The properties of these different models are discussed below.

(i) MODELS WHICH RETAIN THE AMINO ACID ACCEPTOR STEM (H_{33}), ANTICODON STEM (H_{11}), AND THE TψC STEM (H_{29}). In view of the suggestion that the difference between the N and D conformers is due in part to the loss of the DHU stem (Uhlenbeck *et al.*, 1972) (and possibly the minor stem), we first consider all schemes which are consistent with retention of the amino acid acceptor stem (H_{33}), the anticodon stem (H_{11}), and the TψC stem (H_{29}). Examination of the base-pairing matrix reveals that only

TABLE VII: Some Properties of Helices Which are Compatible with the Amino Acid Acceptor Stem (H_{33}), the Anticodon Stem (H_{11}), and the TψC Stem (H_{29}).

	Properties		
Helix No.	Adds Intensity Around 14.0 ppm	Adds no Intensity Around 13.0 ppm	Leaves DHU Loop and Stem Bases Free
H_3	No	No	No
H_4	No	No	No
H_5	No	No	No
H_{13}	Yes?	No	No
H_{19}	No	No	No
H_{21}	Yes?	No	Yes
H_{22}	No	No	Yes
H_{41}	Yes?	No	No

eight other helices might be present, and these are listed in Table VII. In each case we have indicated whether or not the new resonances which are brought in by each of these helices would, in conjunction with the loss of the minor loop stem and DHU stem, provide a reasonable account of the D–N difference spectrum, and whether or not they would be consistent with the oligonucleotide binding data of Uhlenbeck *et al.* (1972). With each model it was necessary to make some assumption as to whether or not the TψC and the amino acid acceptor arm are stacked, and both possibilities were examined. Even with this option we were unable to obtain an acceptable fit of the D–N difference spectrum by any of these models as the comparisons shown in Figure 13 indicate. This applies specifically to one previously proposed model ($H_{33} + H_{29} + H_{11} + H_{22}$) (Webb and Fresco, 1973). In contrast to the *observed* difference spectrum which shows a *gain* of intensity at 14 ppm, this particular model predicts there may be no change or even a *loss* of intensity in this region depending upon the stacking of the TψC and the amino acid acceptor arm. Furthermore, the loss of intensity (two resonances) is too small (experimentally there is a loss of about 4–5) in the 13-ppm region.

Because of the poor fit of the D–N difference spectrum which is obtained with these models, other possible pairing schemes with different initial restrictions were examined. Some guidance as to which features should be included in the model are suggested by a comparison of the N and D

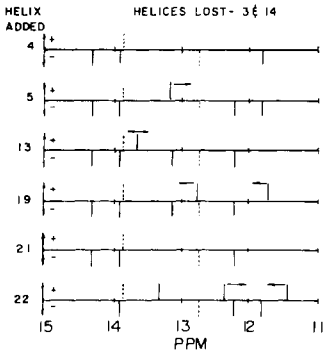

FIGURE 13: Predicted D–N difference spectra for a set of models in which the DHU stem (H_3) and the minor stem (H_{14}) are lost and replaced by one of the helices indicated on the left-hand side of the figure. Compare these results with spectrum shown in Figure 3. The positions of some resonances are sensitive to stacking of helices and the probable range is indicated by arrows.

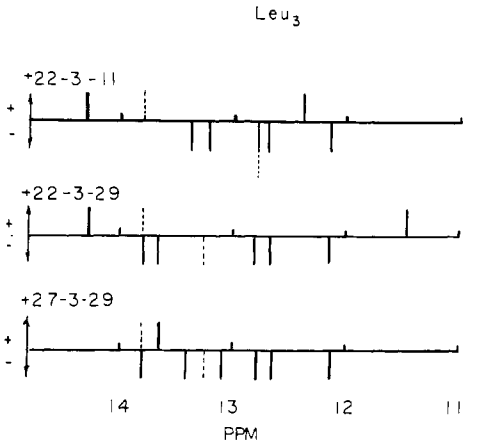

FIGURE 14: Predicted D–N difference spectra for some models which involve loss of the DHU (H_3) stem and either the anticodon stem (H_{11}) or the TψC stem (H_{29}) (see text). The top spectrum is the one computed for the model adopted in the text. The other two models are discussed in the Appendix.

conformer spectra. We note that the same two lowest field resonances appear to be present in both conformers, and, the assignment data presented in Table III indicate these are due to AU_3 in the amino acid acceptor stem and AU_{47} in the minor stem of the N conformer. This suggests that these two stems are also present in the D conformer.

(ii) MODELS CONTAINING THE AMINO ACID (H_{33}), MINOR STEM (H_{14}), AND ANTICODON STEMS (H_{11}) BUT NOT TψC STEM: ($H_{11} + H_{14} + H_{33}$). The helices which are compatible with H_{11}, H_{14}, H_{33} are H_3, H_4, H_5, H_{19}, H_{22}, H_{27}. The first four are eliminated by the requirement that the DHU loop and stem regions be single stranded. The possible pairing schemes are then: $H_{11} + H_{14} + H_{33} +$ (H_{22} or H_{27}) and the difference spectra computed for these models are shown in Figure 14. Neither of these models can account for the increase in the intensity both near 14.0 and 12.5 ppm and on this basis appear to be considerably less adequate than the model shown in Figure 9.

(iii) MODELS WHICH RETAIN ONLY THE AMINO ACID ACCEPTOR STEM H_{33}. As soon as the minor stem is lost there is the problem that in order to account for the ob-

TABLE VIII: A Matrix Illustrating the Compatibility of Helices which Add Resonances to the Low-Field (13–14 ppm) Region of the Nmr Spectrum and Which are Compatible with the Amino Acid Acceptor Stem (H_{33}).[a]

	12	14	17	21	22	25	26	27	32	29	30	41
12		X	X		X							
14	X			X			X				X	X
17	X				X					X		
21		X			X							
22	X		X	X			X					
25							X	X		X	X	X
26		X			X	X		X		X	X	
27						X	X			X	X	
32												
29			X			X	X	X			X	
30		X				X	X	X				
41		X				X						

[a] Incompatibilities are indicated by an X.

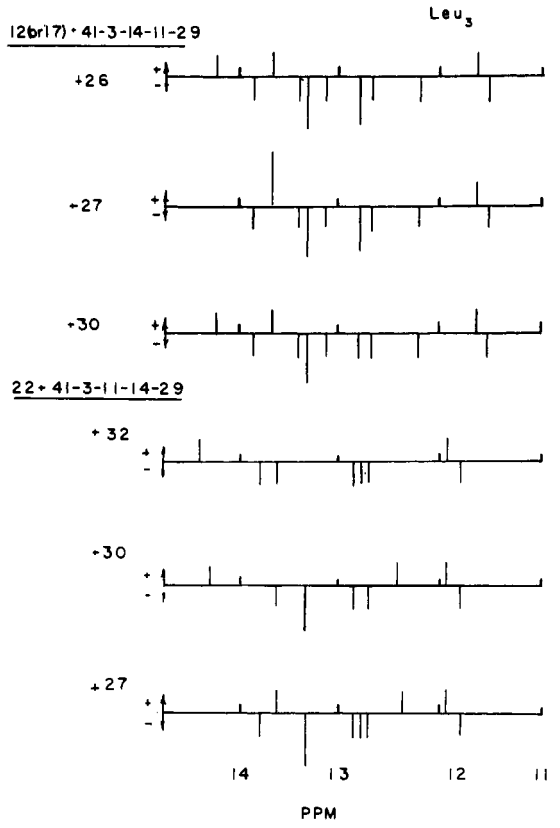

FIGURE 15: Predicted D–N difference spectra for a set of models which involve loss of the DHU stem, minor stem, anticodon stem, and the TψC stem (see Appendix).

served difference spectrum the resonances at 14.3 and 13.9 ppm (which are presumably due to this helix) must be replaced, and a third resonance must be added in this region. Therefore, in attempting to construct a model which lacks the minor stem we look for helices which would provide for these missing low-field resonances. A scan of the possible helices generated the list of helices shown in Table VIII in the form of a compatibility matrix. Two general schemes can be constructed. One group contains the following helices: H_{33} + (H_{12} or H_{17}) + (H_{26}, H_{27} or H_{30}) + H_{41}. These models have six or seven fewer base pairs than the cloverleaf structure whereas experimentally the difference is only 3. Of the six possible schemes, scheme (H_{12} or H_{17}) + H_{33} + H_{41} + H_{30} gives the best fit of the D–N difference spectrum as indicated in Figure 15.

A second set of schemes consistent with the above conditions are based on the following helices: H_{33} + H_{22} + H_{41} + (H_{27}, H_{30} or H_{32}), and the corresponding D–N difference spectra predicted for these schemes are also presented in Figure 15. H_{22} has four base pairs, and therefore should be more stable than either H_{12} or H_{17} of the first set of schemes. Both H_{33} and H_{22} were also used in the scheme shown in Figure 9. H_{30} involves pairing of half of the bases from the original TψC stem with bases from the original minor loop, and resonances originally provided by the minor stem are now provided by H_{41}. Of these latter three schemes, the best fit of the spectrum is obtained when H_{26} or H_{30} are used (see Figure 15) but only the scheme with H_{30} has the proper number of base pairs (18 compared with 16 for the other two schemes).

(iv) MODELS CONTAINING THE AMINO ACID STEM (H_{33}), THE TψC STEM (H_{29}), AND THE MINOR STEM. This is the model which was adopted and it is discussed in the text.

Added in Proof

Recent studies of Hawkins and Chang on the reaction of kethoxal with $tRNA^{Leu}_3$ support the conclusions reached in this paper with regard to the structure of the native and denatured conformers.

References

Chang, S. H., Kuo, S., Hawkins, E., and Miller, N. (1973b), *Biochem. Biophys. Res. Commun. 51,* 951–955.

Chang, S. H., Kuo, S., Miller, N., and Hawkins, E. (1973a), *Fed. Proc., Fed. Amer. Soc. Exp. Biol. 32,* 2272.

Crothers, D. M., Hilbers, C. W., and Shulman, R. G. (1973), *Proc. Nat. Acad. Sci. U. S. 70,* 2899–2901.

Fresco, J. R., Adams, A., Ascione, R., Henley, D., and Lindahl, T. (1966), *Cold Spring Harbor Symp. Quant. Biol. 31,* 527–538.

Gartland, W. T., and Sueoka, N. (1966), *Proc. Nat. Acad. Sci. U. S. 55,* 948–956.

Gralla, J., and Crothers, D. M. (1973), *J. Mol. Biol. 73,* 497–511.

Henley, D. D., Lindahl, T., and Fresco, J. R. (1966), *Proc. Nat. Acad. Sci. U. S. 55,* 191–198.

Kearns, D. R., Lightfoot, D. R., Wong, K. L., Wong, Y. P., Reid, B. R., Shulman, R. G., and Cary, L. (1973), *Ann. N. Y. Acad. Sci. 222,* 324–336.

Kearns, D. R., and Shulman, R. G. (1974), *Accounts Chem. Res. 7,* 33–39.

Kearns, D. R., Wong, Y. P., Hawkins, E., and Chang, S. H. (1974), *Nature (London) 247,* 541–543.

Lightfoot, D. R., Wong, K. L., Kearns, D. R., Reid, B. R., and Shulman, R. G. (1973), *J. Mol. Biol. 78,* 71–89.

Lindahl, T., Adams, A., and Fresco, J. R. (1966), *Proc. Nat. Acad. Sci. U. S. 55,* 941–948.

Lindahl, T., Adams, A., Geroch, M., and Fresco, J. R. (1967), *Proc. Nat. Acad. Sci. U. S. 57,* 178–185.

Muench, K. H. (1969), *Biochemistry 8,* 4880–4888.

Reisner, D., and Römer, R. (1973), *in* Physico-chemical Properties of Nucleic Acids, Vol. 2, Duchesne, J., Ed., London, Academic Press, pp 237–318.

Shulman, R. G., Hilbers, C. W., Kearns, D. R., Reid, B. R., and Wong, Y. P. (1973a), *J. Mol. Biol. 78,* 57–69.

Shulman, R. G., Hilbers, C. W., Wong, Y. P., Wong, K. L., Lightfoot, D. R., Reid, B. R., and Kearns, D. R. (1973b), *Proc. Nat. Acad. Sci. U. S. 70,* 2042–2045.

Streek, R. E., and Zachau, H. G. (1971), *FEBS (Fed. Eur. Biochem. Soc.) Lett. 13,* 329–334.

Tinoco, I., Jr., Uhlenbeck, O. C., and Levine, M. D. (1971), *Nature (London) 230,* 362–367.

Uhlenbeck, O., Chrikjian, J. G., and Fresco, J. R. (1972), *Fed. Proc., Fed. Amer. Soc. Exp. Biol. 31,* 420.

Webb, P. K., and Fresco, J. R. (1973), *J. Mol. Biol. 74,* 387–402.

Wong, K. L., and Kearns, D. R. (1974), *Biopolymers 13,* 371–380.

Wong, Y. P., Kearns, D. R., Reid, B. R., and Shulman, R. G. (1972), *J. Mol. Biol. 72,* 725–740.

Wong, Y. P., Kearns, D. R., Shulman, R. G., Yamane, T., Chang, S., Chrikjian, J. G., and Fresco, J. R. (1973), *J. Mol. Biol. 74,* 403–406.